Biochemistry and Biophysics Reports 39 (2024) 101741

Contents lists available at ScienceDirect

Biochemistry and Biophysics Reports

journal homepage: www.elsevier.com/locate/bbrep

GPC3-targeted CAR-M cells exhibit potent antitumor activity against hepatocellular carcinoma

Lili Guan [a,1], Shanshan Wu [a,**,1], Qinyao Zhu [a], Xiaofang He [c], Xuelong Li [a], Guangqi Song [c], Luo Zhang [d,***], Xiushan Yin [a,b,*]

[a] Applied Biology Laboratory, College of Environmental and Safety Engineering, Shenyang University of Chemical Technology, Shenyang, 110142, China
[b] Suzhou RocRock No.1 Biotechnology Co., Ltd, Suzhou, 215000, China
[c] PuHeng Biotechnology (Suzhou) Co., Ltd, Suzhou, 215000, China
[d] Research Center of Bioengineering, The Medical Innovation Research Division of Chinese PLA General Hospital, Beijing, 100853, China

ARTICLE INFO

Keywords:
GPC3
CAR-M
Hepatocellular carcinoma

ABSTRACT

Chimeric antigen receptor (CAR)-modified macrophages are a promising treatment for solid tumor. So far the potential effects of CAR-M cell therapy have rarely been investigated in hepatocellular carcinoma (HCC). Glypican-3 (GPC3) is a biomarker for a variety of malignancies, including liver cancer, which is not expressed in most adult tissues. Thus, it is an ideal target for the treatment of HCC. In this study, we engineered mouse macrophage cells with CAR targeting GPC3 and explored its therapeutic potential in HCC. First, we generated a chimeric adenoviral vector (Ad5f35) delivering an anti-GPC3 CAR, Ad5f35-anti-GPC3-CAR, which using the CAR construct containing the scFv targeting GPC3 and CD3ζ intracellular domain. Phagocytosis and killing effect indicated that macrophages transduced with Ad5f35-anti-GPC3-CAR (GPC3 CAR-Ms) exhibited antigen-specific phagocytosis and tumor cell clearance in vitro, and GPC3 CAR-Ms showed significant tumor-killing effects and promoted expression of pro-inflammatory (M1) cytokines and chemokines. In 3D NACs-origami spheroid model of HCC, CAR-Ms were further demonstrated to have a significant tumor killing effect. Together, our study provides a new strategy for the treatment of HCC through CAR-M cells targeting GPC3, which provides a basis for the research and treatment of hepatocellular carcinoma.

1. Introduction

According to the data derived from WHO, liver cancer will cause more than 1 million deaths by 2030 [1]. Hepatocellular carcinoma (HCC) is the main histologic type of liver cancer, accounting for about 90 % of liver cancer cases [2,3]. Liver transplantation is currently the best treatment for HCC [4], while advanced HCC still has a fatal prognosis [5]. The significant intrinsic resistance through systemic chemotherapy is mainly due to the phenotypic and molecular heterogeneity of these tumors [6]. So far, commonly used systemic therapeutic agents include two tyrosine kinase inhibitors (TKI), sorafenib and lenvatinib, which have been approved by the US Food and Drug Administration (FDA) [7,8] - as first line systemic therapies for advanced HCC [9]. TKI regorafenib [10] can significantly improve overall survival (OS) as a second line treatment in patients who have previously received sorafenib [6]. Subsequently, a combination of targeted drugs and immune checkpoint inhibitors (ICIs) can provide a synergistic effect, such as atezolizumab plus bevacizumab, which is a breakthrough in the field of HCC treatment [3]. Some novel therapies for the treatment of advanced HCC are under clinical research, which can be divided into three main categories: molecular-targeted monotherapies, immuno-oncology monotherapies and combination therapies. Despite the encouraging progress, there are some therapeutic limitations such as providing limited clinical benefit, development of drug resistance, and the presence of higher synergistic toxicity and lower likelihood of durable efficacy [3,11,12]. Currently, adoptive cell transfer therapy is an emerging and

* Corresponding author. Applied Biology Laboratory, College of Environmental and Safety Engineering, Shenyang University of Chemical Technology, Shenyang, 110142, China.
** Corresponding author.
*** Corresponding author.
E-mail addresses: 1213513231@qq.com (S. Wu), marbleluo@126.com (L. Zhang), xiushanyin@me.com (X. Yin).
[1] These authors contributed to this work equally as co-authors.

https://doi.org/10.1016/j.bbrep.2024.101741
Received 14 March 2024; Received in revised form 10 May 2024; Accepted 23 May 2024
Available online 30 May 2024

promising field of immunotherapy.

GPC3 is a member of the glypican family, representing a glycosylphosphatidylinositol (GPI)-anchored proteoglycan on the cell membrane of cancer cells, which control cell division and growth regulation [13,14]. More than 70 % of HCC had high expression of GPC3, which is not expressed in normal adult tissues [15–17]. Studies have shown that the higher the expression of GPC3 in tumor cells, the worse the prognosis of HCC [14,18,19]. At present, clinical drug development for GPC3 is mainly at clinical phase I. The types of drugs involved include antibody drugs such as codrituzumab [20] as well as ERY974 [21], and CAR-T therapies with limited effective outcome [22].

CAR-M cell therapy has remarkable advantages in the treatment of solid tumors [23,24]. It is difficult for T cells to enter the tumor environment due to vasculature restrictions or physical barriers formed by stroma around tumor cells [25], while macrophages can obviously infiltrate into the tumor environment. And tumor-associated macrophages (TAMs) play an important role in tumor invasion, metastasis, immunosuppression and angiogenesis. CAR-Ms can convert TAMs bystander M2 state into M1 phenotype, so it has a positive boosting effect on the treatment of solid tumors [26]. In addition, CAR-Ms have the function of promoting antigen presentation and enhancing T cell killing [27–29] which makes CAR-M therapy poteintially superior to CAR T therapy. The Gill team from the Perelman School of Medicine at the University of Pennsylvania has proposed that macrophages engineered with chimeric antigen receptors could offer an effective means of treating solid tumors. In vitro, the construction of a THP-1 cell line targeting mesothelin-chimeric antigen receptor (CAR-meso-ζ) can effectively phagocytic mesothelin-positive K562 cells, indicating its phagocytic effect on antigen-positive target cells. Subsequently, They investigated the antitumor activity of the primary human anti-HER2 CAR-M in an in vivo xenograft model, demonstrating that infusion of human CAR-M reduced tumor load and extended overall survival [26]. Similar to CAR-Ts, the CAR structure of CAR-Ms is composed of extracellular signaling domains that recognize specific tumor antigens, transmembrane regions, and intracellular activation signaling regions which activate the phagocytosis of macrophages [30]. Moreover, it has been reported that after intravenous injection of exogenous macrophages in mice, a large proportion of CAR-Ms remains in the liver, which is likely to be beneficial for the treatment of HCC [26]. These combined mechanisms suggest that CAR-M therapy might be potentially more effective against HCC.

Here, we engineered an GPC3-targeted CAR RAW264.7 with adenovirus and evaluated the phagocytic activity against GPC3 positive liver tumor cells. Furthermore, the antitumor effects of GPC3 CAR-M cells were verified by 3D NACs-origami spheroid [31–33]. This study provides a new and effective strategy for the treatment of hepatocellular carcinoma.

2. Materials and methods

2.1. Cell culture and treatment

The cells used here, including HepG2/RAW264.7/293FT/C3A/Huh7, were all originated from ATCC. HepG2 and RAW264.7 cells were cultured in RPMI 1640 medium (Corning, 10-040-CVR) supplemented with 10 % Fetal Bovine Serum (FBS). Huh7 and 293FT cell lines were sustained in Dulbecco' s modified Eagle' s medium (DMEM) (Corning, 10-013-CV) with 10 % FBS. C3A cell lines were cultured in Minimum Essential Medium (MEM) (Gibco, C12571500BT) with 10 % FBS. These cells were all cultured in an incubator at 37 °C with 5 % CO_2.

2.2. Generation of recombinant adenoviruses

Adenoviral transduction of RAW264.7 cells was performed. First, the extracted plasmid without endotoxin was linearized through Pac I digestion at 37 °C, followed by ethanol precipitation for recovery. Subsequently, the recovered plasmid was used for adenoviral packaging. The day before, 293A cells were seeded in a six-well plate, and when the confluence of 293A reached 70 %, adenoviral packaging was performed using the method as indicated in the specification of JetPRIME (Polyplus). Adenovirus was collected after cells were cultured until red fluorescence and cytopathic effects (CPE) were observed. After centrifugation at 2000 rpm for 5 min, the supernatant was discarded, and the cells were resuspended with medium. The suspension underwent three freeze-thaw cycles in a −80 °C freezer, following by centrifugation at 2000*g* for 10 min. The supernatant was collected, filtered through a 0.45 μm membrane, and the viral stock was stored at −80 °C for future use. RAW 264.7 cells were counted for 300,000 and plated into three wells of a six-well plate. The cells were cultured in RMPI 1640 medium containing 10 % FBS and 1 % penicillin.

2.3. Western blot

The expression of GPC3 in hepatocellular carcinoma cell lines was detected by Western blot. RIPA Buffer containing protease inhibitor was used on ice to fully lysate cells, and then centrifuged at 12000 rpm for 10 min, supernatant was added to Loading Buffer, and samples were cooked before loading electrophoresis. The protein was transferred to PVDF membrane by wet transfer system, which was incubated with anti-GPC3 antibody (Abcam, ab174851) overnight at 4 °C. Next, the secondary antibody was incubated at room temperature. Exposure and imaging with ECL reagent.

2.4. Flow cytometry

After 48 h of adenovirus infection, RAW264.7 limited to 1 million were resuspended with PBS adding 1 μl of CD16/CD32 Monoclonal Antibody for blocking at 4 °Cfor 30 min. After that, 1 μl of FITC-labeled G4S antibody (CST, 50515S) was added, and incubated at 4 °C in the dark for 30 min. Ultimately, CAR expression in Ad5f35-transduced RAW264.7 was determined by flow cytometry with 500 μl PBS system. The expression of GPC3 in 293FT/Huh7/HepG2/C3A cells was detected by flow cytometry. The four cell types were enumerated, resuspended in 100 μl of PBS, and exposed to a non-fluorescently labeled GPC3 flow cytometry antibody (Abcam, ab174851) at a 1:50 dilution, maintained at 4 °C for 40 min. Subsequently, the cells underwent three washes with PBS and were centrifuged at 300 g for 3 min. Following primary antibody incubation, a fluorescent secondary antibody (BOSTER,BA1150) was applied at a 1:50 dilution and incubated at 37 °C for 40 min. After the completion of the secondary antibody incubation, the cells were centrifuged, resuspended in 500 μl of PBS, and analyzed by flow cytometry.

2.5. Determination of phagocytosis effect

Huh7/HepG2/C3A cells with positive expression of GPC3 were selected as target cells, and 293FT cells without GPC3 expression were used as negative controls. Un-transduced macrophages (UTD), macrophages transduced with Ad5f35-empty (Empty) were stained with Celltracker Red dye (Invitrogen) as well as staining the target cells including Huh7/HepG2/C3A/293FT with Celltracker Green dye (Invitrogen), respectively. After 24 h, macrophages and tumor cells were co-cultured for 6 h with a ratio of 1:3, and the phagocytosis efficiency was performed with flow cytometry. The percentage of FITC events in the APC population is plotted as the percentage of phagocytosis. The statistical significance between them was calculated using the *t*-test analysis.

2.6. Tumor killing assay

Detection based on fluc killing test: HepG2-fluc, C3A-fluc, Huh7-fluc and macrophages transduced with Ad5f35-anti-GPC3-CAR (GPC3 CAR-

Table 1
Primer sequence list of macrophage M1 and M2 markers was detected by qPCR.

Target	Sequence	NCBI Sequence reference	Length (bp)	TM (°C)
mCCL2 F	CCACAACCACCTCAAGCACT	NM_011333.3	20	60.47
mCCL2 R	AGGCATCACAGTCCGAGTCA	NM_011333.3	20	60.90
mIL1β F	AGAGCTTCAGGCAGGCAGTA	XM_006498795.5	20	60.91
mIL1β R	AGGTGCTCATGTCCTCATCC	XM_006498795.5	20	59.16
mIL6 F	CCAGTTGCCTTCTTGGGACT	NM_001314054.1	20	59.89
mIL6 R	GGTCTGTTGGGAGTGGTATCC	NM_001314054.1	21	59.79
mNOS2 F	CAGCTGGGCTGTACAAACCTTT	NM_001313922.1	22	61.34
mNOS2 R	CATTGGAAGTGAAGCGTTTCG	NM_001313922.1	21	58.43
mTNF-α F	ACGGCATGGATCTCAAAGAC	NM_001278601.1	20	57.97
mTNF-α R	GTGGGTGAGGAGCACGTAGT	NM_001278601.1	20	61.53
mCXCL2 F	GCTGTCCCTCAACGGAAGAA	NM_009140.2	20	59.97
mCXCL2 R	CAGGTACGATCCAGGCTTCC	NM_009140.2	20	59.89
mIL2 F	TTGTGCTCCTTGTCAACAGC	NM_008366.3	20	58.98
mIL2 R	CTGGGGAGTTTCAGGTTCCT	NM_008366.3	20	58.93
mIL18 F	GACAGCCTGTGTTCGAGGAT	XM_036154619.1	20	59.75
mIL18 R	GGTGGATCCATTTCCTCAAAGG	XM_036154619.1	22	58.97
mCD80 F	TGCTGCTGATTCGTCTTTCAC	XM 030248945.2	21	59.20
mCD80 R	GAGGAGAGTTGTAACGGCAAG	XM 030248945.2	21	58.66
mTGF-β F	CCACCTGCAAGACCATCGAC	NM_011577.2	22	61.02
mTGF-β R	CTGGCGAGCCTTAGTTTGGAC	NM_011577.2	22	61.27
mArg-1 F	AACGGGAGGGTAACCATAAGC	NM_007482.3	21	59.79
mArg-1 R	TGATGCCCCAGATGGTTTTC	NM_007482.3	20	58.15
mCD206 F	TTCGGTGGACTGTGGACGAGCA	NM_008625.2	22	66.06
mCD206 R	ATAAGCCACCTGCCACTCCGGT	NM_008625.2	22	66.00
mYm1 F	TGGAATTGGTGCCCCTACAA	NM_009892.4	20	59.22
mYm1 R	CCACGGCACCTCCTAAATTG	NM_009892.4	20	58.91
mVEGFA F	GACTATTCAGCGGACTCACCA	NM_001025257.3	20	59.52
mVEGFA R	TGAGGGAGTGAAGAACCAACC	NM_001025257.3	20	59.58
mPD-L1 F	TGCTGTCACTTGCTACGGG	NM_021893.3	19	60.01
mPD-L1 R	GTCCAGCTCCCGTTCTACAG	NM_021893.3	20	59.83

Ms) were co-cultured in 96-well cell culture plates for luciferase-based killing experiments. The effector-to-target (E:T) ratios were 1:1 and 2:1, respectively. Bioluminescence was measured using a microplate reader. By the following formula, calculating the percentage of specific kills based on the luciferase signal (total flux) relative to individual tumors before normalization. Detection based on LDH killing test: C3A and Huh7 tumor cells cultured alone were used as controls, then co-culturing C3A and Huh7 with GPC3 CAR-Ms for LDH-based killing assays. After 3

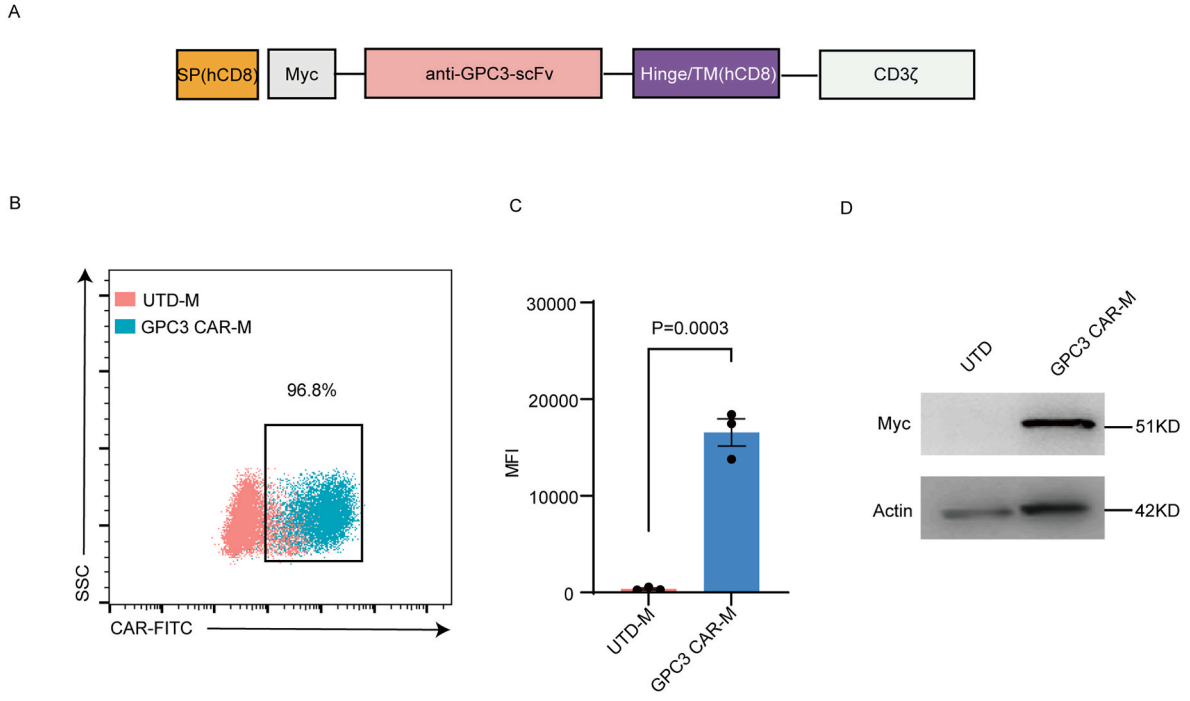

Fig. 1. Generation of GPC3-targeted RAW264.7 CAR-M cells after adenoviral transduction.
(A). Schematic diagram of anti-GPC3 CAR structure. (B). Flow cytometry was used to detect the expression of CAR in RAW264.7 infected with Ad5f35-GPC3-CAR for 48 h, G4S-FITC Linker monoclonal antibodies target scFv-based CAR, UTD was labeled with G4S antibody as a negative control. (C). The expression intensity of CAR was evaluated by FACS, corresponding to the results of (B), data are represented MFI. UTD as a negative control. (D). Analysis of the protein expression of Myc-tag in CAR-M cells by Western blot.

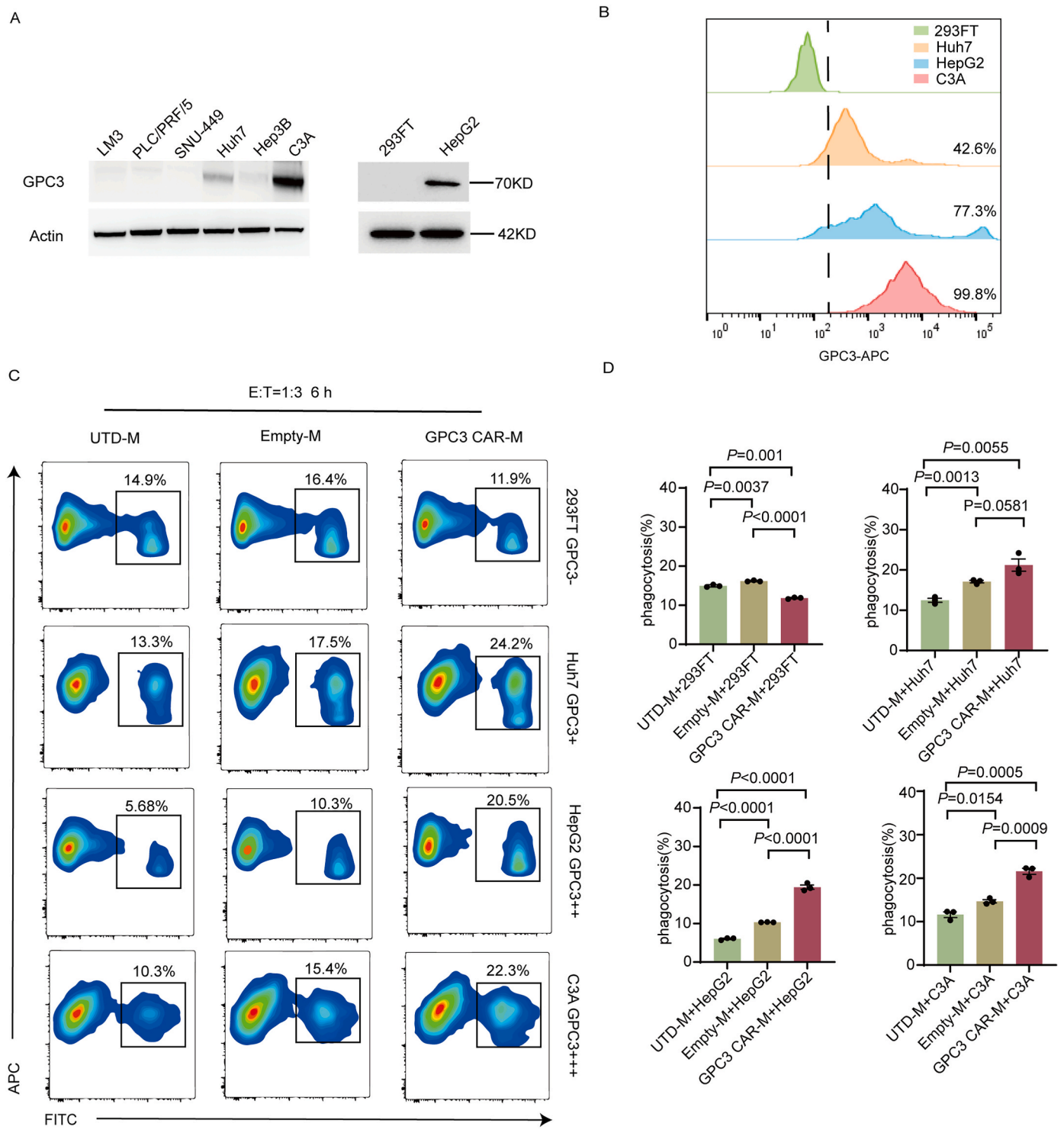

Fig. 2. Evaluation of phagocytic efficacy in vitro with different GPC3 positive cells.
(A). Western blot analysis was performed to detect the expression of GPC3 protein in human hepatoma cell lines including LM3, PLC/PRF/5, SNU-449, Huh7, Hep3B, C3A and HepG2, as well as 293FT. (B). Flow cytometry was used to detect the expression of GPC3 protein in Huh7, HepG2, C3A and 293FT in human hepatocellular carcinoma cell lines. (C). Phagocytic effect of UTD/Empty/GPC3 CAR-M targeting 293FT/Huh7/HepG2/C3A were analyzed by FACS for 6 h at an E:T ratio of 3:1. (D). The evaluation of macrophage phagocytosis against 293FT/Huh7/C3A/HepG2 cells was performed through flow cytometry. The data, presented with n = 3, illustrate the observed phagocytic activity. Data were represented as the mean ± s.e.m. from n = 3 technical replicates. Statistical significance was calculated using a two-tailed *t*-test.

h, the supernatant was transferred to a 96-well plate and sequentially added substrate reaction solution and stop solution in the LDH Assay kit. Measure the absorbance at 490 nm using a microplate reader.

2.7. Validation of CAR-M targeting and cytotoxicity in a 3D NACs-origami spheroid

The 3D NACs-origami spheroid was constructed with C3A-fluc cells.

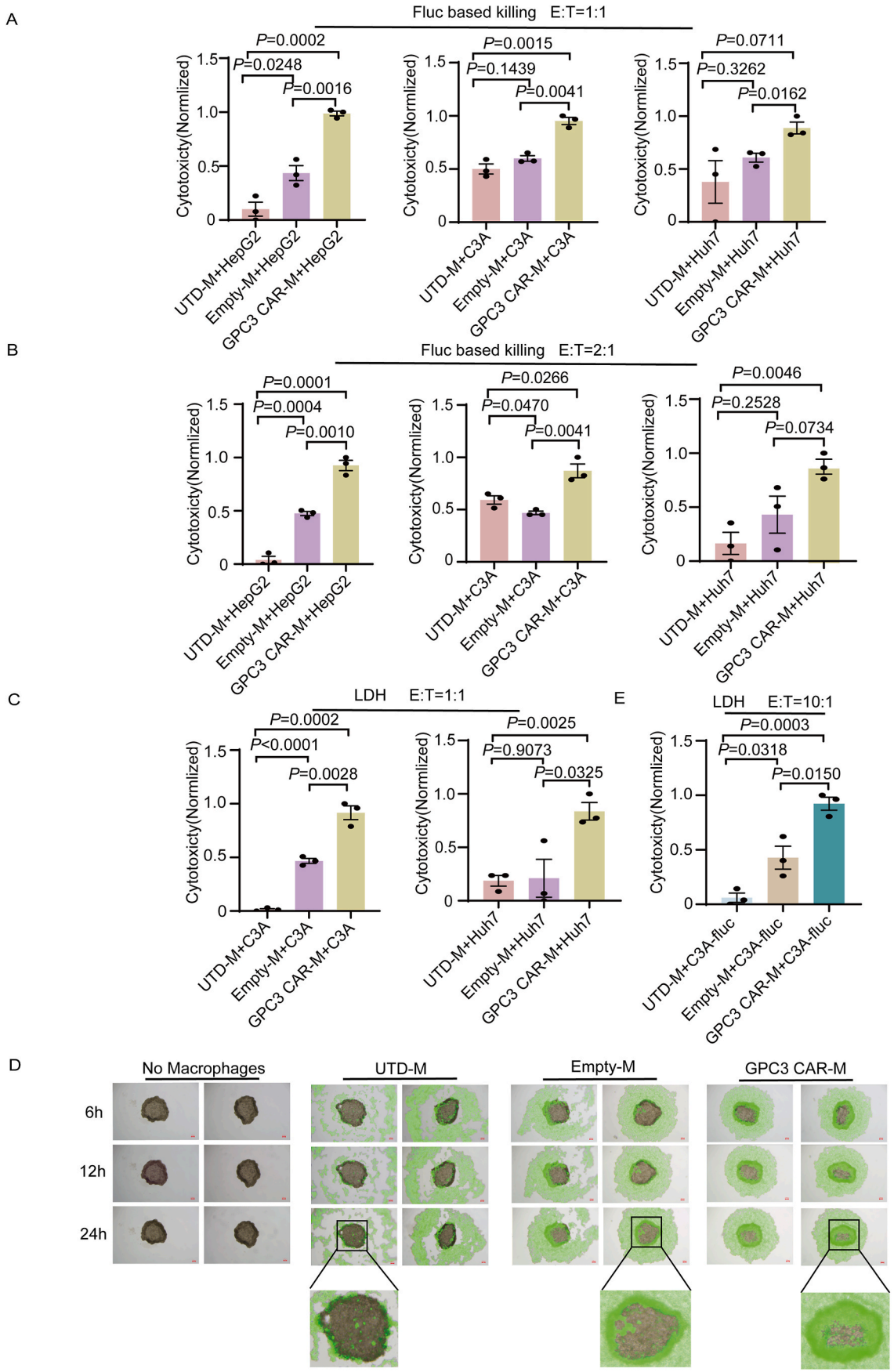

(caption on next page)

Fig. 3. Evaluation of the killing ability in 2D and 3D NACs-origami spheroid.
(A). The killing effect of HepG2 and C3A as well as Huh7 co-cultured with GPC3 CAR-Ms at E:T ratio of 1:1 for 24 h in vitro was evaluated. UTD and Empty were used as control groups. Data are represented as the mean ± s.e.m. from n = 3 technical replicates. Statistical significance was calculated using a two-tailed *t*-test. (B). Fluc based killing assay of E:T ratio at 2:1. (C). C3A and Huh7 were used as target cells to evaluate the LDH-based killing effect of GPC3 CAR-Ms, which were co-cultured for 3 h with E:T ratio of 1:1. UTD and Empty served as the control group. (D). Constructing 3D NACs-origami spheroid with C3A-fluc cells to further verify the antitumor effect of GPC3 CAR-Ms. Co-cultures were established with UTD, Empty-M, and GPC3 CAR-M at an effector-to-target (E:T) ratio of 10:1 with the 3D NACs-origami spheroid, and the field and fluorescence images were taken at 6 h, 12 h and 24 h, respectively. (E). LDH assay was performed at 12 h. The absorbance at 490 nm was measured by microplate reader.

UTD and Empty and CAR-M cells were stained with Celltracker Green dye and photographed at 6 h, 12 h, and 24 h, respectively. After 12 h, the Cytotoxicity LDH Assay Kit-WST® was utilized to perform a quantitative analysis of the lactate dehydrogenase activity in the cell culture supernatant, in order to assess the extent of cellular damage. First, the Assay Buffer from the kit was added to the Dye Mixture and thoroughly mixed to prepare the substrate reaction solution. Next, the cell supernatant was added into the 96-well plate at the rate of 1:1 to the substrate reaction solution. After 10 min of reaction, 25 μL stopping solution was added to stop the reaction. The absorbance at 490 nm was measured with a microplate reader and normalized after the following treatment.

2.8. RNA extraction and qPCR analysis

Total RNA was extracted from cells using the Eastep® Super Total RNA Extraction Kit (Promega). RNA was reverse-transcribed with random primers, which was carried out using the HiScript III 1st Strand cDNA Synthesis Kit (Vazyme), and qPCR was performed in triplicate using AceQ qPCR SYBR Green Master Mix (Without ROX) (Vazyme) on CFX Connect Real-Time System (BIO-RAD). All experiments were performed in accordance with the manufacturers' instructions. The forward and reverse primers used for the validation of macrophage M1 and M2 types were presented in Table 1.

2.9. Statistical analysis

The data analysis was conducted utilizing GraphPad Prism 9.5 software, and the findings were reported as mean ± Standard Error of Mean. Comparative analysis between the two groups was performed using independent sample t-tests for statistical assessment. A p-value less than 0.05 was considered statistically significant.

3. Results

3.1. GPC3 CAR-Ms expressed CAR with high efficiency

To demonstrate the potential of CAR-mediated macrophage-specific phagocytosis, we transduced RAW264.7 cells using an anti-GPC3 CAR structure encoding anti-GPC3 single-chain fragment variable (scFv) and CD3ζ intracellular domain, and Myc-tag was designed behind the N-terminal signal peptide of the CAR fragment. (Fig. 1A). Significant expression of CAR in the GPC3 CAR-M cells reached 96.8 % after transducing macrophages with adenovirus (Fig. 1B and C), and Myc expression was detected by WB to determine CAR expression (Fig. 1D). Overall, our data proved that GPC3 CAR-Ms expressed CAR with high efficiency.

3.2. GPC3 CAR-Ms showed antigen-dependent phagocytic effect on GPC3 positive cells

We validated the targeted phagocytosis function of CAR by in vitro phagocytosis experiments with Ad5f35-transduced RAW264.7 on positive cells with different levels of GPC3 antigen expression. Meanwhile, we constructed an adenoviral vector lacking CAR structure as control named Ad5f35-Empty. First, we screened seven human hepatoma cell lines and chose Huh7/HepG2/C3A as GPC3 positive target cells and 293FT as GPC3 negative target cell (Fig. 2A). Next, we used flow cytometry to further detect the expression of GPC3 in these four cells and performed subsequent in vitro phagocytosis experiments (Fig. 2B). After co-culturing Ad5f35-transduced RAW264.7 with C3A/Huh7/HepG2/293FT for 6 h respectively, we observed that the phagocytotic efficiency of GPC3 CAR-M was significantly higher compared to Empty and UTD when the target cells were GPC3-positive, while there was no significant difference when the target cells were 293FT GPC3-negative (Fig. 2C and D). Huh7 phagocytosis with low GPC3 expression was comparable to the highest expressed cell lines, like C3A and HepG2, indicating that the CAR was extremely sensitive. Even for low or medium expressed cells. Together, we demonstrated the ability of GPC3 CAR-mediated antigen specific and sensitive phagocytosis.

3.3. GPC3 CAR-Ms exhibited significant antitumor effects against liver cancer cells

To further validate the efficacy of CAR, we assessed the cytotoxic capabilities of GPC3 CAR-Ms against the aforementioned cell lines. In initial experiments, we established an effector to target (E:T) ratio of 1:1 for cytotoxicity detection based on fluc activity. The findings demonstrated that GPC3 CAR-Ms exhibited significant cytotoxic effects across all three GPC3-expressing cell lines when compared to the control group (Fig. 3A). Subsequently, the E:T ratio was adjusted to 2:1, and the results further confirmed the sensitivity and specific cytotoxic potential of GPC3 CAR-Ms (Fig. 3B). Additionally, the specific cytotoxicity of GPC3 CAR-Ms on hepatocellular carcinoma (HCC) cell lines was evaluated by measuring LDH release. We selected the C3A cell line with the highest GPC3 expression and the Huh7 cell line with the lowest expression for LDH-based cytotoxicity experiments at an E:T ratio of 1:1. The outcomes indicated that both Huh7 and C3A cell lines were similarly affected, further corroborating the target specificity and sensitivity of GPC3 CAR-Ms (Fig. 3C).

NACs-organ was a 3D microtumor spheroid models that utilize biomolecular materials in conjunction with DNA origami technique, enabling the distinctive 3D growth environment of tumors. Recently, we utilized this technique to validate the infiltrative and cytotoxic capabilities of CAR-M. To validate the cytotoxic capabilities of CAR-Ms, the 3D NACs-origami spheroid was constructed by C3A-fluc with an effector-to-target ratio of 10:1. It became evident that CAR-M cells increasingly gathered and permeated the 3D tumor spheroid model, which revealed the robust targeting recruitment and infiltration capabilities of CAR-M within this model (Fig. 3D). We assessed the killing ability of CAR at 12 h by LDH, confirming apparently cytotoxicity of CAR-M against 3D tumor spheroids than control groups (Fig. 3E). Above all, we claimed that CAR-M cells had a potent antitumor effect in the treatment of HCC.

3.4. GPC3 CAR-Ms transformed into a M1 pro-inflammatory phenotype

After determining that CAR-M cells had robust phagocytosis and killing effect on GPC3-positive tumor cells, we assessed whether CAR-transduced macrophages induced a pro-inflammatory (M1) macrophage phenotype, utilizing the qPCR system. The results showed that all M1-related factors were up-regulated, including CCL2, IL1β, IL6, NOS2, TNF-α, CXCL2, IL2, IL18, and CD80, while M2-related factors were down-regulated in CAR-transduced macrophages compared to the UTD group, such as TGF-β, Arg-1, CD206, Ym1, VEGFA, and PD-L1. This

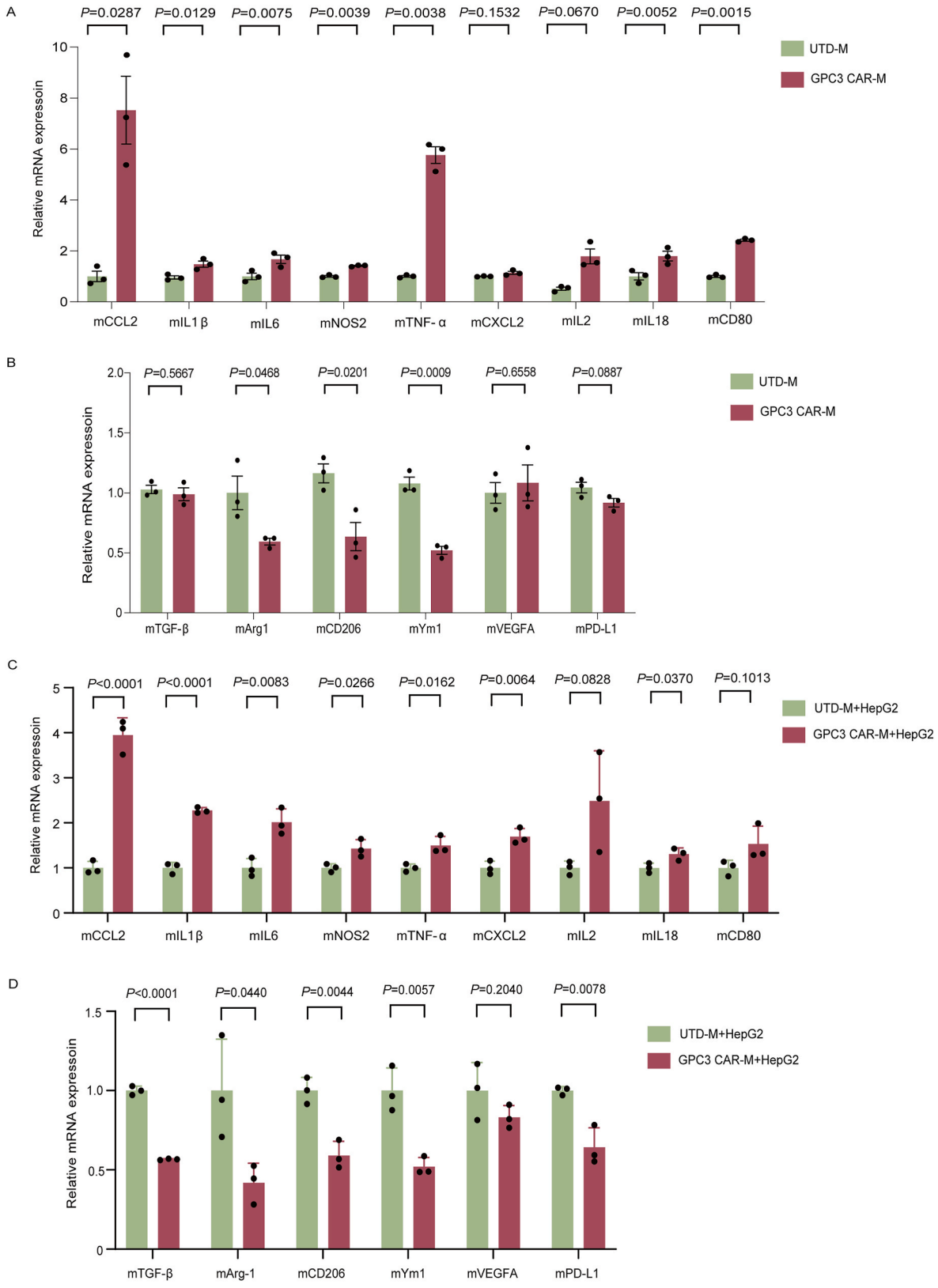

Fig. 4. The mRNA expression levels of M1 and M2 related genes were detected by qPCR.
(A). qPCR was performed to detect the mRNA expression of M1-type (classically activated macrophage) cytokines in CAR-Ms and UTDs. (B). Detection of M2-type (alternatively activated macrophage) cytokines mRNA expression in CAR-Ms and UTDs by qPCR. (C). The mRNA expression of M1-type cytokines was detected by qPCR after co-culturing of CAR-Ms and UTDs with HepG2 for 6 h with E:T ratio of 1:3, respectively. (D). qPCR was performed to detect the mRNA expression of M2-type cytokines after co-culturing of CAR-Ms and UTDs with HepG2 for 6 h with E:T ratio of 1:3, respectively. Data are represented as the mean ± sem. from n = 3 technical replicates. Statistical significance was calculated using a two-tailed *t*-test.

suggests that CAR-transduced macrophages were polarized toward the M1 phenotype (Fig. 4A and B). Further, we evaluated alterations in both the anti-tumor M1 phenotype and the pro-tumor development-associated M2 phenotype of GPC3 CAR-M cells during co-cultivation. After co-culturing UTD/GPC3 CAR-Ms with HepG2 for 6 h, we collected cells to determine the expression of M1/M2 phenotype related factors. The results revealed a significant upregulation of M1-related factors in GPC3 CAR-Ms during co-cultivation with HepG2 compared to the UTD. Correspondingly, M2-related factors in GPC3 CAR-Ms exhibited a significant downregulation compared to UTD. (Fig. 4C and D). Therefore, compared to UTD, GPC3 CAR-Ms were reprogrammed into a M1 proinflammatory phenotype at the transcriptome level. Together, these data demonstrated GPC3 CAR could polarize macrophages towards the M1 phenotype regardless of whether it was in a co-culture system, further demonstrating its anti-tumor potential.

4. Discussion

In recent years, macrophages have emerged as prominent candidates for the treatment of solid tumors used in immunotherapy. As innate immune cells, macrophages have a wide range of therapeutic effects, including active infiltration to tumor sites, direct phagocytosis of targeted tumors, activation of tumor microenvironment and professional antigen presentation. Tumor-associated macrophages (TAMs) can be classified into M1-type and M2-type macrophages based on their activation types and distinct roles in tumors [34]. The presence of M2-type tumor-associated macrophages (TAMs) promotes the onset and progression of tumors. Recently, research has revealed that chimeric adenoviral vectors overcome the innate resistance of macrophages to genetic manipulation and reprogram the state towards an M1 phenotype [26]. Therefore, adenovirus was selected to deliver GPC3-CAR to macrophages to assess the therapeutic effect of hepatocellular carcinoma in this study.

The results of this study demonstrated that GPC3-positive cells such as HepG2/Huh7/C3A were sensitive to CAR-M cells compared with GPC3-negative cells 293FT. Next we further confirmed that CAR-Ms exerted potent antitumor effects in 3D NACs-origami spheroid of HCC·In summary, we verified that Ad5f35-transduced RAW264.7 targeted GPC3 exhibited antigen-specific phagocytosis and tumor cell clearance in vitro and endowed macrophages with a persistent proinflammatory (M1) phenotype. This study provides evidence for the treatment of hepatocellular carcinoma with GPC3-related immunotherapy at cellular level, and opens a new avenue for clinical treatment of liver cancer.

CRediT authorship contribution statement

Lili Guan: Writing – original draft, Methodology, Formal analysis, Data curation. **Shanshan Wu:** Writing – review & editing, Data curation. **Qinyao Zhu:** Data curation. **Xiaofang He:** Methodology. **Xuelong Li:** Methodology. **Guangqi Song:** Methodology. **Luo Zhang:** Writing – review & editing. **Xiushan Yin:** Writing – review & editing, Resources, Conceptualization.

Declaration of competing interest

The authors declare that they have no known competing financial interests or personal relationships that could have appeared to influence the work reported in this paper.The authors declare the following financial interests/personal relationships which may be considered as potential competing interests:

All responding author reports financial support was provided by National Natural Science Foundation of China, 2023 Ganzhou City Technology Innovation Center and so on. Xiushan Yin, Shanshan Wu, Lili Guan has patent pending to Suzhou Kunshi No.1 Biotechnology Co., Ltd. X. H. and G. S. are the employee of Puheng Technology Co., Ltd. The other authors declare no personal financial conflict of interest. If there are other authors, they declare that they have no known competing financial interests or personal relationships that could have appeared to influence the work reported in this paper.

Acknowledgements

This research project was funded by the National Natural Science Foundation of China [32371490], and supported by Shenyang University of Chemical Technology-Roc Rock Biotechnology (Suzhou) Co., Ltd joint research grant [2021210101004606], and supported by 2023 Ganzhou City Technology Innovation Center [2023ZXGX7956], and 2023 National Center for Biotechnology Innovation in Cellular Therapy "Unveiling and Commanding" Technology Research Project - Macrophage Drug Development Targeting Solid Tumors [2023XB0010] to Xiushan Yin.

Appendix A. Supplementary data

Supplementary data to this article can be found online at https://doi.org/10.1016/j.bbrep.2024.101741.

References

[1] A. Villanueva, Hepatocellular carcinoma, N. Engl. J. Med. 380 (15) (2019) 1450–1462, https://doi.org/10.1056/NEJMra1713263.
[2] J.M. Llovet, R.K. Kelley, A. Villanueva, et al., Hepatocellular carcinoma, Nat. Rev. Dis. Prim. 7 (1) (2021) 6, https://doi.org/10.1038/s41572-020-00240-3.
[3] C. Yang, H. Zhang, L. Zhang, et al., Evolving therapeutic landscape of advanced hepatocellular carcinoma, Nat. Rev. Gastroenterol. Hepatol. 20 (4) (2023) 203–222, https://doi.org/10.1038/s41575-022-00704-9.
[4] C.H. Patt, P.J. Thuluvath, Role of liver transplantation in the management of hepatocellular carcinoma, J. Vasc. Intervent. Radiol. 13 (9 Pt 2) (2002) S205–S210, https://doi.org/10.1016/s1051-0443(07)61788-6.
[5] A. Vogel, A. Cervantes, I. Chau, et al., Hepatocellular carcinoma: ESMO Clinical Practice Guidelines for diagnosis, treatment and follow-up, Ann. Oncol. 29 (4) (2018) iv238–iv255, https://doi.org/10.1093/annonc/mdy308.
[6] A. Vogel, A. Saborowski, Current strategies for the treatment of intermediate and advanced hepatocellular carcinoma, Cancer Treat Rev. 82 (2020) 101946, https://doi.org/10.1016/j.ctrv.2019.101946.
[7] J.M. Llovet, S. Ricci, V. Mazzaferro, et al., Sorafenib in advanced hepatocellular carcinoma, N. Engl. J. Med. 359 (4) (2008) 378–390, https://doi.org/10.1056/NEJMoa0708857.
[8] M. Kudo, R.S. Finn, S. Qin, et al., Lenvatinib versus sorafenib in first-line treatment of patients with unresectable hepatocellular carcinoma: a randomised phase 3 non-inferiority trial, Lancet 391 (10126) (2018) 1163–1173, https://doi.org/10.1016/S0140-6736(18)30207-1.
[9] K. Du, Y. Li, J. Liu, et al., A bispecific antibody targeting GPC3 and CD47 induced enhanced antitumor efficacy against dual antigen-expressing HCC, Mol. Ther. 29 (4) (2021) 1572–1584, https://doi.org/10.1016/j.ymthe.2021.01.006.
[10] J. Bruix, S. Qin, P. Merle, et al., Regorafenib for patients with hepatocellular carcinoma who progressed on sorafenib treatment (RESORCE): a randomised, double-blind, placebo-controlled, phase 3 trial, Lancet 389 (10064) (2017) 56–66, https://doi.org/10.1016/S0140-6736(16)32453-9.
[11] J. Boshuizen, D.S. Peeper, Rational cancer treatment combinations: an urgent clinical need, Mol. Cell 78 (6) (2020) 1002–1018, https://doi.org/10.1016/j.molcel.2020.05.031.
[12] A.L. Cheng, Y.K. Kang, A.R. He, et al., Safety and efficacy of tigatuzumab plus sorafenib as first-line therapy in subjects with advanced hepatocellular carcinoma: a phase 2 randomized study, J. Hepatol. 63 (4) (2015) 896–904, https://doi.org/10.1016/j.jhep.2015.06.001.
[13] P.Y. Meng, F. Zhang, W. Zhang, et al., Identification of the atypical cadherin FAT1 as a novel glypican-3 interacting protein in liver cancer cells, Sci. Rep. 11 (1) (2021) 40, https://doi.org/10.1038/s41598-020-79524-3.
[14] D. Shi, Y. Shi, A.O. Kaseb, et al., Chimeric antigen receptor-glypican-3 T-cell therapy for advanced hepatocellular carcinoma: results of phase I trials, Clin. Cancer Res. 26 (15) (2020) 3979–3989, https://doi.org/10.1158/1078-0432.CCR-19-3259.
[15] D. Li, J. Qin, T. Zhou, et al., Bispecific GPC3/PD-1 CAR-T cells for the treatment of HCC, Int. J. Oncol. 62 (4) (2023), https://doi.org/10.3892/ijo.2023.5501.
[16] X. Cui, Z. Li, P.J. Gao, et al., Prognostic value of glypican-3 in patients with HBV-associated hepatocellular carcinoma after liver transplantation, Hepatobiliary Pancreat. Dis. Int. 14 (2) (2015) 157–163, https://doi.org/10.1016/s1499-3872(15)60349-6.
[17] Q. Zhang, Z. Han, J. Tao, et al., An innovative peptide with high affinity to GPC3 for hepatocellular carcinoma diagnosis, Biomater. Sci. 7 (1) (2018) 159–167, https://doi.org/10.1039/c8bm01016a.

[18] M. Capurro, I.R. Wanless, M. Sherman, et al., Glypican-3: a novel serum and histochemical marker for hepatocellular carcinoma, Gastroenterology 125 (1) (2003) 89–97, https://doi.org/10.1016/s0016-5085(03)00689-9.
[19] N. Yamauchi, A. Watanabe, M. Hishinuma, et al., The glypican 3 oncofetal protein is a promising diagnostic marker for hepatocellular carcinoma, Mod. Pathol. 18 (12) (2005) 1591–1598, https://doi.org/10.1038/modpathol.3800436.
[20] G.K. Abou-Alfa, O. Puig, B. Daniele, et al., Randomized phase II placebo controlled study of codrituzumab in previously treated patients with advanced hepatocellular carcinoma, J. Hepatol. 65 (2) (2016) 289–295, https://doi.org/10.1016/j.jhep.2016.04.004.
[21] T. Ishiguro, Y. Sano, S.I. Komatsu, et al., An anti-glypican 3/CD3 bispecific T cell-redirecting antibody for treatment of solid tumors, Sci. Transl. Med. 9 (410) (2017), https://doi.org/10.1126/scitranslmed.aal4291.
[22] P. Rochigneux, B. Chanez, B. De Rauglaudre, et al., Adoptive cell therapy in hepatocellular carcinoma: biological rationale and first results in early phase clinical trials, Cancers 13 (2) (2021), https://doi.org/10.3390/cancers13020271.
[23] Y. Chen, Z. Yu, X. Tan, et al., CAR-macrophage: a new immunotherapy candidate against solid tumors, Biomed. Pharmacother. 139 (2021) 111605, https://doi.org/10.1016/j.biopha.2021.111605.
[24] Y. Gao, Y. Ju, X. Ren, et al., Enhanced infection efficiency and cytotoxicity mediated by vpx-containing lentivirus in chimeric antigen receptor macrophage (CAR-M), Heliyon 9 (12) (2023) e21886, https://doi.org/10.1016/j.heliyon.2023.e21886.
[25] M.M. D Aloia, I.G. Zizzari, B. Sacchetti, et al., CAR-T cells: the long and winding road to solid tumors, Cell Death Dis. 9 (3) (2018) 282, https://doi.org/10.1038/s41419-018-0278-6.
[26] M. Klichinsky, M. Ruella, O. Shestova, et al., Human chimeric antigen receptor macrophages for cancer immunotherapy, Nat. Biotechnol. 38 (8) (2020) 947–953, https://doi.org/10.1038/s41587-020-0462-y.
[27] L. Franken, M. Schiwon, C. Kurts, Macrophages: sentinels and regulators of the immune system, Cell Microbiol. 18 (4) (2016) 475–487, https://doi.org/10.1111/cmi.12580.
[28] T.L. Tang-Huau, P. Gueguen, C. Goudot, et al., Human in vivo-generated monocyte-derived dendritic cells and macrophages cross-present antigens through a vacuolar pathway, Nat. Commun. 9 (1) (2018) 2570, https://doi.org/10.1038/s41467-018-04985-0.
[29] D.A. Hume, Macrophages as APC and the dendritic cell myth, J. Immunol. 181 (9) (2008) 5829–5835, https://doi.org/10.4049/jimmunol.181.9.5829.
[30] M.T. Villanueva, Macrophages get a CAR, Nat. Rev. Drug Discov. 19 (5) (2020) 308, https://doi.org/10.1038/d41573-020-00053-9.
[31] J. Wang, H. Du, L. Ma, et al., MitoQ protects ovarian organoids against oxidative stress during oogenesis and folliculogenesis in vitro, Int. J. Mol. Sci. 24 (2) (2023), https://doi.org/10.3390/ijms24020924.
[32] X. Li, M. Zheng, B. Xu, et al., Generation of offspring-producing 3D ovarian organoids derived from female germline stem cells and their application in toxicological detection, Biomaterials 279 (2021) 121213, https://doi.org/10.1016/j.biomaterials.2021.121213.
[33] J. Liu, X. He, Q. Zhu, et al., DNA origami assembled spheroid for evaluating cytotoxicity and infiltration of chimeric antigen receptor macrophage (CAR-M), bioRxiv (2023), https://doi.org/10.1101/2023.12.03.569750.
[34] X. Xiang, J. Wang, D. Lu, X. Xu, Targeting tumor-associated macrophages to synergize tumor immunotherapy, Signal Transduct. Targeted Ther. 6 (1) (2021) 75, https://doi.org/10.1038/s41392-021-00484-9.